

Magnetization-Prepared Cardiac Imaging Using Gradient Echo Acquisition

Yu Liu, Stephen J. Riederer, Richard L. Ehman

Magnetization-prepared 2DFT and 3DFT gradient echo techniques are presented for acquisition of black blood cardiac images. Both methods incorporate RF pulses for blood saturation, centric or centric-like view ordering, data acquisition during late diastole, and breath-holding. In a series of 13 volunteer studies, these methods have consistently provided good visualization of intraventricular structures.

Key words: cardiac MRI; breath hold MRI.

INTRODUCTION

Imaging of the heart with magnetic resonance techniques has been a long-active area of research work. The most successful earliest techniques employed RF refocused spin-echo imaging in conjunction with ECG gating (1). A separate phase encoding measurement of a slice was acquired each cardiac cycle, leading to acquisition times of several minutes depending on resolution and averaging. Although the image quality attainable with this technique may suffer from cardiac arrhythmia, flow, and respiratory motion, RF refocused spin-echo imaging is still regarded by many as the method of choice for routine morphological cardiac imaging.

Gradient echo and echo-planar methods have also been used for cardiac imaging. Gradient echo methods are used principally for assessing dynamic function (2), although such techniques have also been demonstrated in morphologic imaging with sub-second acquisition times (3, 4). Echo-planar methods (5) offer acquisition times of several tens of milliseconds, and hence have an obvious application to cardiac imaging. Results have been demonstrated by several groups (6, 7). However, despite the progress in fast scan techniques, breath-hold methods have not substantially replaced or even supplemented gated spin-echo methods in morphological cardiac imaging. The reasons are likely due to a combination of factors, including inadequate spatial resolution, inadequate signal-to-noise ratio (SNR), poor myocardium-to-chamber contrast and in the case of echo-planar methods, the need for special gradient hardware.

The purpose of this work was to investigate whether these limitations of gradient echo cardiac imaging tech-

niques could be addressed with modification to the pulse sequence. In doing so, acquisition times were allowed for 2DFT imaging which extended over several cardiac cycles but still were within a single 16-sec breath-hold. For further improved spatial resolution, 3DFT methods were developed which extended over 16 breath-holds. In terms of anatomic detail, we believe the images represent a significant improvement over results generated previously with gradient echo and echo-planar techniques and rival high quality gated spin-echo results.

METHODS AND MATERIALS

The 2DFT and 3DFT gradient echo methods are both based on the same pulse sequence, as shown in Fig. 1. At the start of each cardiac cycle a combination of nonselective and selective 180° RF pulses is applied for saturation of blood signal (8). This saturation pulse pair is gated by the ECG signal with a trigger delay T of 100 ms after the R wave. The data acquisition starts TI 300 ms after the saturation pulse pair. At this point the recovering negative longitudinal magnetization of blood approaches zero, and after four dummy repetitions it passes through zero. After the dummy repetitions 16 phase encoding views are acquired. Readout parameters used were 256 points sampled over an echo with a 4-ms duration with a TE of 4.5 ms. With a TR of 10 ms the data acquisition window is 160 ms long and located in the diastolic phase of the cardiac cycle. For a single image a longer data acquisition window than this tends to cause image degradation by cardiac motion, while a shorter window prolongs the total scan time for a given resolution and TR . In the 2D data acquisition, since averaging was deemed necessary for adequate SNR, the phase-offset multiplanar technique (9) was also incorporated for efficiency improvement. Two images at different spatial locations are acquired in a single 16-s breath-hold.

The phase encoding order for the 2DFT acquisition is centrally interleaved in k -space as shown in Fig. 2A. With phase encoding resolution of 128 for each individual image, the equivalent of averaging of two excitations, and assuming incorporation of the POMP technique, the total number of phase encodings acquired is 256. Assuming 16 measurements per cardiac cycle, the total acquisition time is 16 cardiac cycles. As shown in the figure, in each cycle, phase encodings are sampled every 8th starting from the center of k -space and interleaved with those sampled in other cycles. Because the low absolute value k_y views are sampled earliest within each cardiac cycle, contrast between myocardium and chamber caused by the RF pulse pair and TI delay tends to be preserved (10).

In an attempt to get superior SNR to that provided by the 2DFT technique with averaging, 3DFT techniques were also considered (11). 3DFT MRI acquisition has

JMRI 30:271-275 (1993)

From the Magnetic Resonance Research Laboratory, Department of Diagnostic Radiology, Mayo Clinic, Rochester, Minnesota (Y.L., S.J.R., R.L.E.); and Biomedical Engineering Department, Duke University, Durham, North Carolina (Y.L.).

Address correspondence to: Stephen J. Riederer, Ph.D., MR Research Laboratory, Department of Diagnostic Radiology, Mayo Clinic, Rochester, MN 55905.

Received February 19, 1993; revised April 22, 1993; accepted April 22, 1993.

0740-3194/93 \$3.00

Copyright © 1993 by Williams & Wilkins

All rights of reproduction in any form reserved.

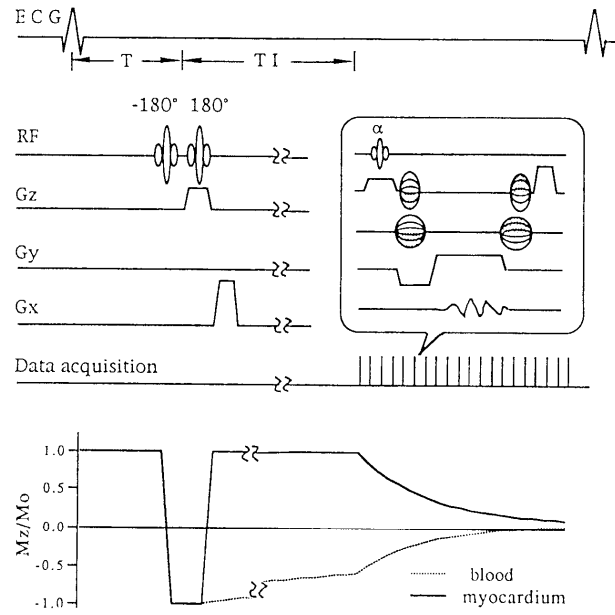


FIG. 1. Schematic diagram for cardiac imaging data acquisition pulse sequences and time course of the longitudinal magnetization for myocardium and blood. $T = 150$ ms, $T_I = 300$ ms, $TR/TE = 10/4.5$ ms, and flip angle 30° . The acquisition pulse sequence enclosed by line is repeated 20 times with four dummy repetitions and 16 measurements.

potentially higher SNR and spatial resolution than 2DFT acquisition, but typically requires a longer scan time. The specific technique used was determined as follows. We assumed that the in-plane resolution was a minimum of $128_y \times 256_x$, and that a minimum of 16-slice partitions would be used. This requires a total of 2048 phase encodings. Similar to the 2DFT case described above, if 16 measurements are made per cardiac cycle, then imaging must occur for 128 cardiac cycles. Because multiple breath-holds are required for such an acquisition, the time per breath-hold was relaxed from the 16 cardiac cycles used for the 2DFT case to eight cardiac cycles. This causes the number of breath-holds to be 16. There is a 4-s pause between each breath-hold. Thus the total acquisition time is approximately 3 min. The volumes excited by the blood saturation pulse are superior and inferior to the imaging slices and are partially overlapped with the 3D slab. The four outer slices located at each side of the 16-slice 3D slab are discarded because they are saturated by the RF blood saturation pulses. The readout parameters used for the 3DFT technique were the same as for the 2DFT case.

The phase encoding view order used for the 3DFT acquisition is illustrated in Fig. 2B, a plot of k_y - k_z space. The order is based on central ordering of views for 3DFT acquisition of magnetization not at steady state (12). Each echo is represented by a point in the plot, and constitutes a sample along the k_x direction, orthogonal to the plane of the plot.

Although 128 cardiac cycles are used in the actual 3DFT acquisition, for the purpose of illustration the Fig. 2B plot assumes only 16 cardiac cycles. All phase encodings which are to be measured are first assigned along an

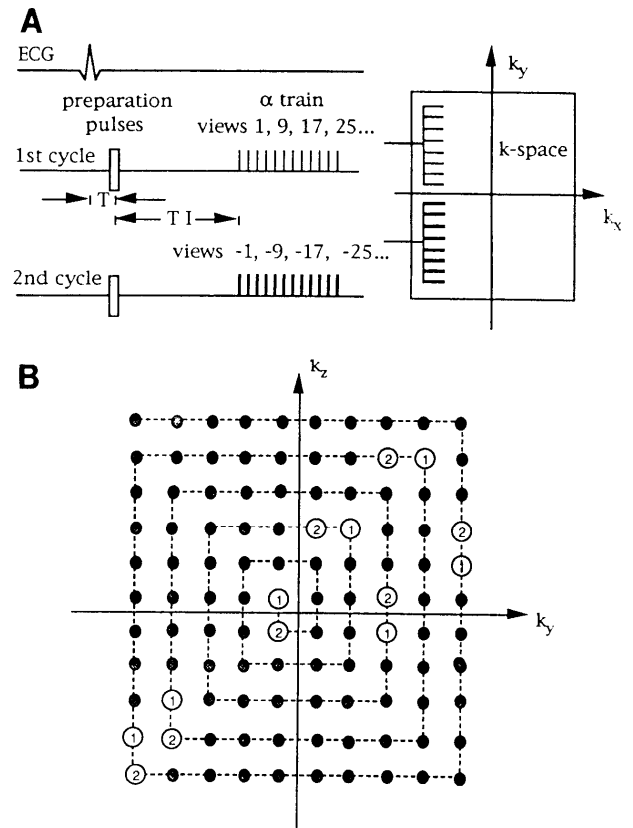


FIG. 2. (A) Schematic of 2DFT data acquisition order for ECG gated breath-hold short TR cardiac imaging. In each cardiac cycle, data acquisition starts from the center of k -space and phase encoding views acquired from different cycles are interleaved. The view numbers represent actual view locations in the k -space. (B) Data acquisition in 3D k -space. Each \bullet represents a phase encoding view along k_x . $\textcircled{1}$, views acquired in the 1st cardiac cycle; $\textcircled{2}$, views acquired in the 2nd cycle. In each cardiac cycle, data acquisition starts from center of the k_y - k_z plane along a trajectory drawn by dashed line. For the purpose of illustration, a scan time spanning a total of only 16 cardiac cycles is assumed.

outwardly expanding square spiral, starting at or near the origin of k_y - k_z space. Measurements made during a single cardiac cycle sample widely spaced points along this square spiral trajectory, the spacing being equal to the total number of cardiac cycles used. For example, the first measurement of the first cardiac cycle samples the point designated $\textcircled{1}$ near the origin of Fig. 2B, the next measurement samples the next point so designated along the spiral, positioned in the first quadrant 16 points further along the trajectory. This continues until all 16 measurements are made for the first cardiac cycle. For the second cardiac cycle the process is similar and starts with the first point along the spiral which has not yet been sampled. Just as for the 2DFT case, this sampling scheme ensures that the central phase encodings of k_y - k_z space are measured when the myocardium-blood contrast is highest, at the outset of the data acquisition of Fig. 1.

Human studies were performed in seven volunteers using the 2DFT method and in six volunteers using the

3DFT techniques described above. All images were acquired on a 1.5 T commercial MR scanner (GE Signa, Milwaukee, WI) equipped with standard gradient hardware. A four-element phased array multicoil was used for improved SNR compared with that provided by the standard body coil. During the scan the volunteer was positioned supine and in the head first position. The field-of-view (FOV) was 280 mm. For the 2DFT acquisition the slice thickness was 8 mm and the slab thickness not affected by the blood saturation pulses was 16 mm. For the 3DFT acquisition a slab thickness of 64 mm was used with 16 partitions, so each slice was 4 mm thick. For purposes of comparison, gated spin-echo images were also acquired on some volunteers with the parameters: TE = 11 ms, acquisition matrix 128×256 , FOV 280 mm, slice thickness 8 mm, 2 NEX, and trigger delay 500 ms. Respiratory artifacts were reduced by respiratory-ordered phase encoding. TR was selected to be equal to the R-to-R interval, which varied modestly from volunteer to volunteer but was typically just less than 1000 ms. Acquisition times were 4.5 min with 2 NEX.

The 2DFT and 3DFT gradient echo images were evaluated by the authors with careful attention paid to the depiction of intraventricular structure, myocardium to blood contrast, and prominence of any artifacts.

RESULTS

Shown in Fig. 3 are 2DFT gradient echo images acquired in sagittal and coronal planes. Intraventricular structures such as the right ventricle (RV) trabeculae are clearly delineated (a, black arrow). The right coronary artery (RCA) is seen in the coronal image (b, white arrow).

In vivo images acquired from another volunteer using the conventional gated spin-echo techniques (a), the described 2DFT (b), and 3DFT gradient echo techniques (c)-(f) are shown in Fig. 4. The direction of slice select in 2DFT and slab select in 3DFT case is anterior-posterior. In (a) left and right ventricles are shown in the gated spin-echo image. There are some flow artifacts in the phase encoding direction, although blood saturation is used. In (b) cardiac anatomy is revealed very well, respiratory artifact is eliminated because of breath-holding, and flow artifact is suppressed by effective saturation of blood. Intraventricular structures such as the papillary

muscles (d, arrow) are depicted with high resolution in images of the contiguous sections in (c)-(f). The endocardial surface is modestly better defined in (c)-(f) than (b) because the slice thickness is now 4 versus 8 mm for the 2DFT case.

Cardiac images (3DFT) acquired in the sagittal plane of another volunteer are shown in Fig. 5. Excellent resolution of the cardiac chambers is seen in all of images. The left and right ventricles are depicted very well, with clear delineation of small structures such as the papillary muscles (b, arrow) and trabeculae (c, arrow). These structures are often poorly visualized in gated spin-echo images.

In the volunteer studies, both the 2DFT and 3DFT gradient echo techniques consistently provided good quality results. All seven 2DFT studies were successful in that intraventricular structures were visualized, intraventricular blood was well saturated, and respiratory artifacts as manifested by ghosting were negligible. Similarly, the six 3DFT studies were also considered to be of good quality using the same criteria. Only one of the six 3DFT studies was modestly degraded by ghosting artifact, most likely due to some lack of consistency of the breath-hold position.

DISCUSSION

We have demonstrated high resolution imaging of the heart using 2DFT and 3DFT short TR gradient echo techniques. We believe that the results presented demonstrate an improvement in SNR and spatial resolution compared to results presented previously with gradient echo techniques. Based on the resolution with which intraventricular structures, such as the papillary muscles, moderator band, and trabeculae, are seen, the image quality even rivals that of conventional spin-echo imaging.

For the 2DFT case the improvement in image quality over single shot methods (3, 4) is due to several factors. First, the acquisition time has been extended from one to several cardiac cycles, but still within a breath-hold. This increase in time allows 256×128 resolution and signal averaging. Second, the RF pulse pair and TI delay provide good myocardium-to-blood contrast. Third, the centric view order preserves this contrast in the resultant image.

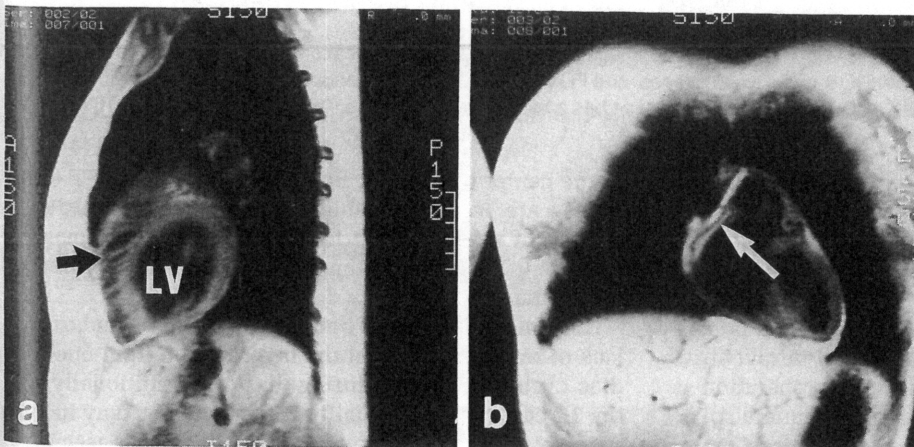


FIG. 3. 2DFT cardiac images acquired using breath-hold gradient echo techniques. Images are acquired in 16 s. Small structures such as RV trabeculae (black arrow) and the right coronary artery (white arrow) are clearly depicted.

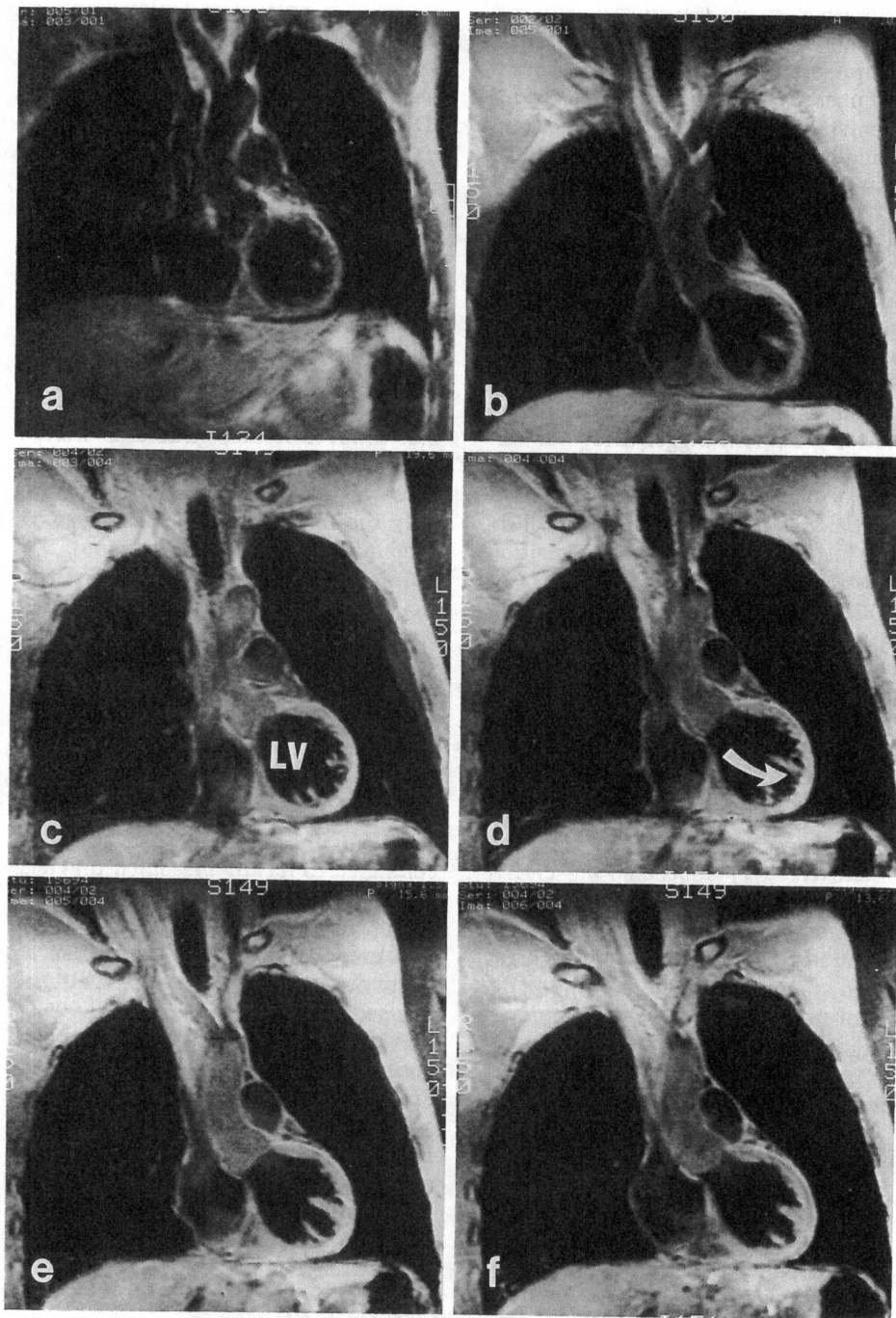


FIG. 4. (a) is gated spin-echo image and (b) is 2DFT gradient echo image acquired at the same location for comparison. Parameters of 2D acquisition are: 128×256 resolution, 2 NEX, 8-mm slice thickness, and FOV 280 mm. From posterior to anterior, (c)–(f) are contiguous *in vivo* coronal cardiac images acquired using 3DFT technique. Each slice has a thickness of 4 mm in a slab of 64 mm thick with 16 partition. Papillary muscle is indicated by the arrow.

By extension of the acquisition time to several breath-holds, 3DFT acquisition is allowed and permits even improved image quality. Specifically, the SNR gain provided by simultaneous acquisition of multiple (in this case 16) sections, more than compensates for the SNR loss in going to a 4-mm section thickness. This is considered to be important in visualizing small intraventricular structures. The same magnetization preparation is used for the 3D as for the 2D case, and the square spiral view order for the 3D case assigns the high contrast views

to the center of k -space. Both the 2DFT and 3DFT techniques are less vulnerable to cardiac arrhythmia and change of cardiac cycle than gated spin-echo imaging because the TR used in the data acquisition is not tied to the cardiac cycle.

Current limitations of both methods are related to any lack of reproducibility of the myocardium from one cardiac cycle to the next during diastole. Additionally, for the 3D case the image quality is susceptible to any inconsistency in gross position of the heart over consecutive

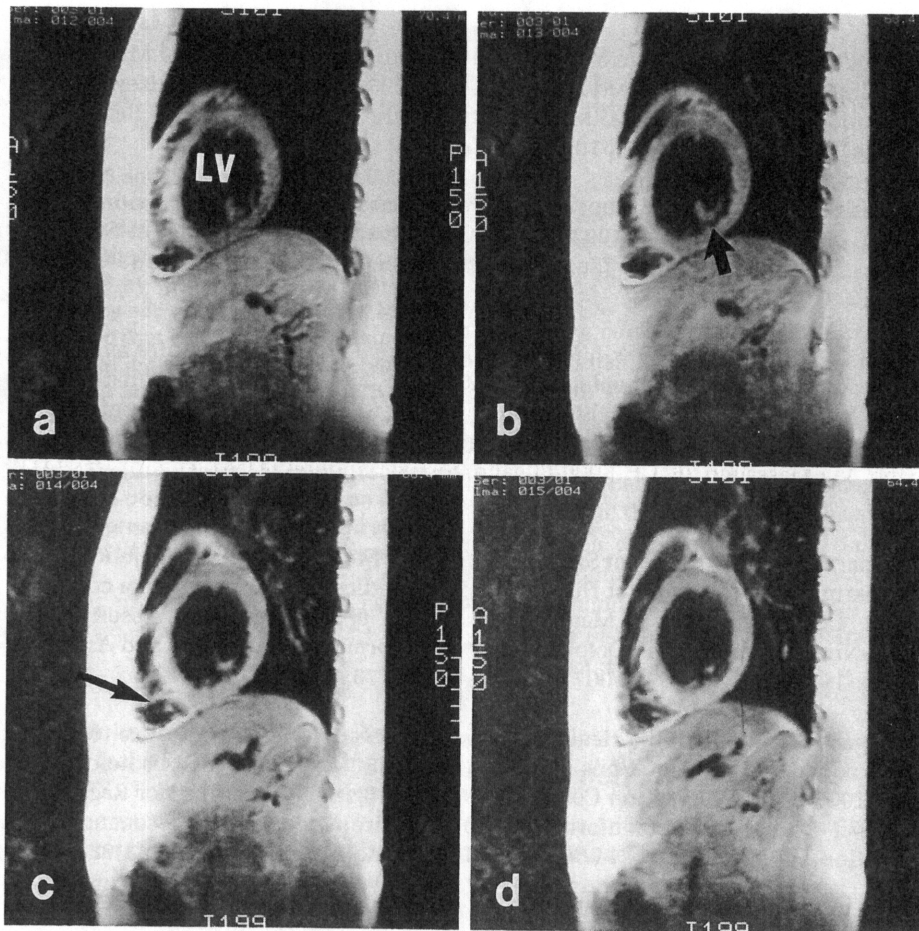


FIG. 5. (a)–(d) contiguous *in vivo* sagittal cardiac images from left to right. They are acquired using the 3D short *TR* gradient echo acquisition. Small structures such as papillary muscles (short arrow) and RV trabeculae (long arrow) are clearly depicted.

breath-holds. Relatively artifact-free images were obtained for five out of six volunteers studied. It remains to be seen whether this level of performance can be attained in clinical studies.

In summary, we have demonstrated that cardiac images providing excellent visualization of intraventricular structures and the endocardial surface can consistently be obtained using breath-hold 2DFT and 3DFT magnetization-prepared gradient echo techniques. These may supplement gated spin-echo techniques for morphological imaging.

ACKNOWLEDGMENTS

We acknowledge the support of NIH Grants CA37993 and HL37310 and of General Electric Medical Systems.

REFERENCES

1. L. E. Crooks, B. Barker, H. Chang, D. Feinberg, J. C. Hoeningner, J. C. Watts, M. Arakawa, L. Kaufman, P. E. Sheldon, E. Botvinick, C. B. Higgins, *Radiology* **153**, 459 (1984).
2. G. H. Glover, N. J. Pelc, in "Magnetic Resonance Annual" (H. Y. Kressel, ed.), pp. 299–333, Raven Press, New York, 1988.
3. J. Frahm, K. D. Merboldt, H. Bruhn, M. L. Gyngell, W. Hancicke, D. Chien, *Magn. Reson. Med.* **13**, 150 (1990).
4. D. Matthaei, A. Haase, D. Henrich, E. Dühmke, *Radiology* **177**, 527 (1990).
5. P. Mansfield, I. L. Pykett, *J. Magn. Reson.* **29**, 355 (1978).
6. R. R. Rzedzian, I. L. Pykett, *AJR* **149**, 245 (1987).
7. B. Chapman, R. Turner, R. J. Ordidge, M. Doyle, M. Cawley, R. Coxon, P. Glover, P. Mansfield, *Magn. Reson. Med.* **5**, 246 (1987).
8. R. R. Edelman, D. Chien, D. Kim, *Radiology* **181**, 655 (1991).
9. G. H. Glover, *J. Magn. Reson. Imaging* **1**, 457 (1991).
10. A. E. Holsinger, S. J. Riederer, *Magn. Reson. Med.* **16**, 481 (1990).
11. Y. Liu, S. J. Riederer, R. L. Ehman, in "Book of Abstracts, 11th Annual Meeting, Society of Magnetic Resonance in Medicine, 1992," p. 2536.
12. H. W. Korin, S. J. Riederer, A. E. H. Bampton, *J. Magn. Reson. Imaging* **2**, 687 (1992).